Rules of selection for spontaneous coherent states in mesoscopic systems: Using the microcavity laser as an analog study

Y. F. Chen,* K. F. Huang, and H. C. Lai
Department of Electrophysics, National Chiao Tung University, 1001 TA Hsueh Road, Hsinchu, Taiwan 30050

Y. P. Lan
Institute of Electro-Optical Engineering, National Chiao Tung University, Hsinchu, Taiwan
(Received 2 April 2003; published 19 August 2003)

The selection rules for spontaneous coherent waves in mesoscopic systems are experimentally studied using the transverse patterns of a microcavity laser and theoretically analyzed using the theory of SU(2) coherent states. Comparison of the experimental results with the theoretical analyses reveals that an amplitude factor A should be included in the representation of the partially coherent states. The determination of the amplitude factor A is found to be associated with the constraint of minimum energy uncertainty.

DOI: 10.1103/PhysRevE.68.026210 PACS number(s): 05.45.−a, 03.65.Ge, 42.55.Sa, 73.23.Ad

Recently, the progress in modern semiconductor technology has made it possible to design nanostructure devices with quantum ballistic properties [1]. The results of recent studies of open square quantum dots show that the striking phenomena of conductance fluctuations are associated with wave patterns localized on classical periodic orbits [2–4]. The general principles of pattern formation indicate that small disturbances can cause the real system to select some states from the range available to the idealized perfect system [5,6]. Although there are mathematically many possible selections, the experimental results reveal that the wave patterns associated with classical periodic orbits are often the persistent states in mesoscopic systems [7–9]. Therefore, to establish the relation between the quantum wave functions and the classical periodic orbits is a crucial phase in investigating the quantum phenomena in mesoscopic systems [10,11]. In this work, we experimentally and theoretically study the selection rules for the spontaneous coherent states associated with the classical periodic orbits in mesoscopic systems.

In recent years, microwave cavities have been used to perform analog studies of transport in open quantum dots [7–9]. More recently, we demonstrated that the transverse patterns of oxide-confined vertical-cavity surface-emitting lasers (VCSEL's) reveal the probability density of the wave functions corresponding to two-dimensional (2D) quantum billiards [12]. Here we use square-shaped VCSEL's with 40 μm oxide aperture to investigate the variations of the transverse pattern with the heat sink temperature. The emission wavelength near the lasing threshold is normally close to the peak gain wavelength, which shifts with temperature (0.2–0.3 nm/K) at a faster rate than does the VCSEL cavity resonance. The transverse-mode spacing can be derived as $\Delta\lambda \approx \lambda^3/(4a^2)$, where $\lambda \approx 780$ nm is the fundamental wavelength and a is the length of the square boundary. Since the transverse-mode spacing is around $\Delta\lambda \approx 0.07$ nm, the transverse patterns of VCSEL's can be easily detuned by controlling the heat sink temperature. Although an ideal 2D square billiard has many possible eigenstates, only a few stationary states are observed in experimental transverse patterns. As shown in Fig. 1, only three types of transverse pattern are usually observed by detuning the temperature from 280 to 240 K. Similar to the quantum flows in open square quantum dots [2–4], the observed transverse patterns of square-shaped VCSEL's are concentrated along classical periodic orbits instead of being regular eigenstates of the perfect square billiard. The present result supports the idea that the properties of the wave functions in mesoscopic structures can be analogously studied by designing optical structures with similar or identical functional forms [13]. Recently, Doya *et al.* [14] introduced the paraxial approximation to establish an analogy between light propagation along a multimode fiber and quantum-confined systems. It is believed that these analogies will continue to be exploited for understanding the physics of mesoscopic systems.

Previously, we analytically constructed the wave functions related to the primitive periodic orbit (p,q,ϕ) in a 2D square billiard by using the representation of SU(2) coherent states, where p and q are two positive integers describing the number of collisions with the horizontal and vertical walls, and the phase factor ϕ $(-\pi \leqslant \phi \leqslant \pi)$ that is related to the wall positions of specular reflection points [15]. As in the Schwinger representation of the SU(2) algebra, the wave

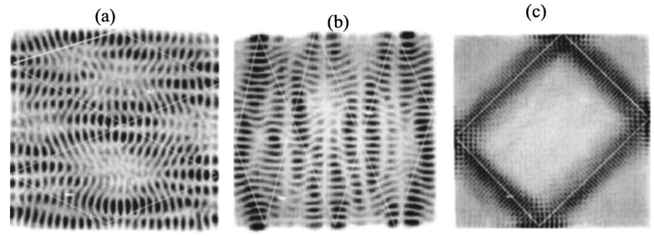

FIG. 1. The experimental near-field patterns of the VCSEL device near the lasing threshold at temperatures around (a) 270–280, (b) 260–270, and (c) 240–260 K. The white lines superimposed on top of the wave patterns indicate the related classical periodic orbits.

*Author to whom correspondence should be addressed. FAX: 886-35 729134. Electronic address: yfchen@cc.nctu.edu.tw

function associated with high-order periodic orbits (p,q,ϕ) is analytically expressed as [15]

$$\Psi_N^{p,q}(x,y;\tau)=\frac{(2/a)}{(1+|\tau|^2)^{N/2}}\sum_{K=0}^{N}\sqrt{C_K^N}\tau^K \times\sin\left[p(K+1)\frac{\pi x}{a}\right]\sin\left[q(N-K+1)\frac{\pi y}{a}\right], \tag{1}$$

where a is the length of the square boundary, N represents the order of the coherent state, K is associated with the order of the eigenstates, C_K^N is the binomial coefficient, and the parameter τ is related to the phase factor ϕ by $\tau=\exp(i\phi)$. The relationship between the parameter ϕ and the periodic orbits can be understood by using the identity $\sin z=(e^{iz}-e^{-iz})/2i$ to rewrite Eq. (1) and applying the property of the *Dirichlet kernel*. A detailed discussion can be found in Ref. [15]. Using Eq. (1) and $|\tau|^2=1$, the ratio of the average speeds along the x and y axes in the classical limit ($N\to\infty$) is found to be p/q. The result of $\sqrt{\langle \nu_x^2\rangle/\langle \nu_y^2\rangle}=p/q$ is consistent with the requirement of classical periodic orbits. On the other hand, $\Delta H/\langle H\rangle$ is inversely proportional to N, where $\langle H\rangle$ is the expectation value of the Hamiltonian and ΔH is the dispersion in energy obtained by computing $\sqrt{\langle H^2\rangle-\langle H\rangle^2}$. Therefore, $\Delta H/\langle H\rangle\to 0$ as $N\to\infty$. This asymptotic property indicates that the coherent states in Eq. (1) are stationary states in the classical limit. However, the coherent state in Eq. (1) for mesoscopic systems, i.e., N is finite, is generally not a stationary state for the Hamiltonian of a perfect square billiard because the eigenstate components are not degenerate.

For mesoscopic systems, the experimental phenomena reveal that the parameter τ should be generalized as $A\exp(i\phi)$, where the amplitude factor A is a positive real value. With $\tau=A\exp(i\phi)$, Eq. (1) becomes

$$\Psi_N^{p,q}(x,y;A,\phi)=\frac{(2/a)}{(1+A^2)^{N/2}}\sum_{K=0}^{N}\sqrt{C_K^N}A^K e^{iK\phi} \times\sin\left[p(K+1)\frac{\pi x}{a}\right] \times\sin\left[q(N-K+1)\frac{\pi y}{a}\right]. \tag{2}$$

It can be found that the coherent states in Eq. (2) have the asymptotic behavior

$$\Psi_N^{p,q}(x,y;A,\phi) \sim\begin{cases}(2/a)\sin(p\pi x/a)\sin[q(N+1)\pi y/a] & (A\to 0),\\ (2/a)\sin[p(N+1)\pi x/a]\sin(q\pi y/a) & (A\to\infty).\end{cases}$$

Nevertheless, the amplitude factor A in the range of 0.1–10 has a great deal to do with the fine structure of wave patterns. It will be demonstrated later that the determination of the amplitude factor A plays an important role in comparing the theoretical calculations with the experimental results. Hereafter the amplitude factor A is considered in the range of 0.1–10 unless otherwise specified.

Comparison of the experimental results with the theoretical analyses reveals that the coherent state in Eq. (2) should be modified to be a partially coherent state that includes 3–7 nearly degenerate eigenstates. In fact, only a few nearly degenerate eigenstates are already sufficient to localize wave patterns on high-order periodic orbits [15]. Moreover, the coherent state in Eq. (2) represents a traveling-wave property. To make a comparison with experimental results, the standing-wave representations can be obtained by replacing the factor $e^{iK\phi}$ by $\sin(K\phi)$ or $\cos(K\phi)$. Accordingly, the partially coherent state can be defined as

$$\Psi_{N,M}^{p,q}(x,y;A,\phi)=\frac{(2/a)}{\left[\sum_{K=K_0-J}^{K_0+J}C_K^N A^{2K}\sin^2(K\phi)\right]^{1/2}} \times\sum_{K=K_0-J}^{K_0+J}\sqrt{C_K^N}A^K\sin(K\phi) \times\sin\left[p(K+1)\frac{\pi x}{a}\right] \times\sin\left[q(N-K+1)\frac{\pi y}{a}\right], \tag{3}$$

where $K_0=[N(A^2/1+A^2)]$, the symbol $[\nu]$ denotes the largest integer $\leqslant\nu$, and the index $M=2J+1$ represents the number of eigenstates used in the state $\Psi_{N,M}^{p,q}(x,y;A,\phi)$. The number of eigenstates M is somewhat restricted because $\Delta H/\langle H\rangle$ is generally proportional to the index M for a given order N. In most cases, experimental results reveal that $3\leqslant M\leqslant 7$. Note that the coefficient $C_K^N A^{2K}$ is associated with the relative probability amplitude of the eigenstate $(2/a)\sin[p(K+1)(\pi x/a)]\sin[q(N-K+1)(\pi y/a)]$ and its value is maximum for $K=K_0$. To be brief, the partially coherent state is a superposition of a few eigenstates next to the eigenstates of maximum probability in the standard SU(2) representation.

As mentioned earlier, the partially coherent states in Eq. (3) are also not stationary states for a perfect square billiard. Nevertheless, the spontaneous symmetry breaking or weak perturbation may cause the partially coherent state to be a stationary state. Since the amplitude factor A has much to do with the fine structure of the wave pattern, it is much more informative to comprehend the A dependence of the energy uncertainty $\Delta H/\langle H\rangle$ for the partially coherent state $\Psi_{N,M}^{p,q}(x,y;A,\phi)$. Figure 2 shows the A dependence of the energy uncertainty $\Delta H/\langle H\rangle$ and several related patterns for the partially coherent state $\Psi_{30,5}^{1,2}(x,y;A,0.47\pi)$. The value of the phase ϕ is determined by the best fit for experimental results. It can be seen that the partially coherent state $\Psi_{30,5}^{1,2}(x,y;A,0.47\pi)$ has a minimum energy uncertainty around $A=2.15$. More importantly, the wave pattern with the minimum energy uncertainty agrees very well with the experimental result depicted in Fig. 1(a).

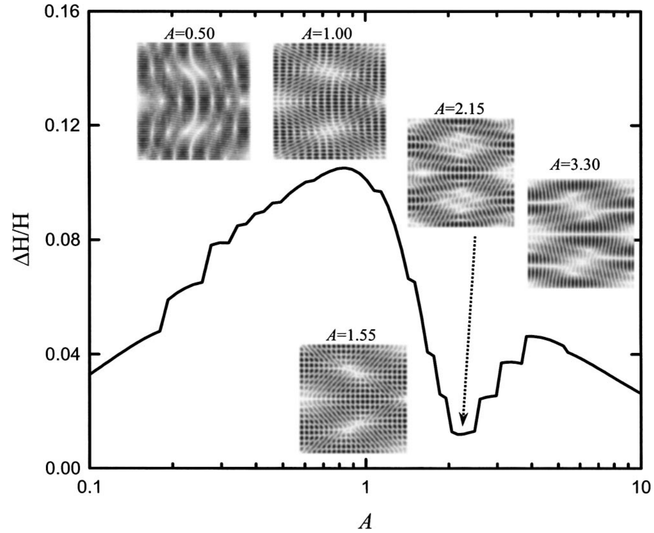

FIG. 2. The calculated results of the A dependence of the energy uncertainty $\Delta H/\langle H\rangle$ for the partially coherent state $\Psi^{1,2}_{30,5}(x,y;A,0.47\pi)$. Several calculated patterns for different values of A are shown in the insets; the calculated pattern with minimum $\Delta H/\langle H\rangle$ corresponds to the experimental result shown in Fig. 1(a).

Similar plots for partially coherent states $\Psi^{3,1}_{29,3}(x,y;A,0.55\pi)$ and $\Psi^{1,1}_{80,7}(x,y;A,0.45\pi)$ are shown in Figs. 3 and 4, respectively. Here again the wave patterns with minimum $\Delta H/\langle H\rangle$ are in good agreement with experimental results shown in Figs. 1(b) and 1(c). Therefore, it can be concluded that the partially coherent states with minimum energy uncertainty in perfect systems usually become the eigenstates in those systems with small disturbances or tiny symmetry breaking. In other words, the wave function obtained as a linear superposition of a few nearly degenerate eigenstates can provide a more physical description of a phenomenon than the true eigenstates in real mesoscopic systems. Even so, the pump profile should be essentially uniform to guarantee that the partially coherent state is the correct criterion for a VCSEL laser just above threshold.

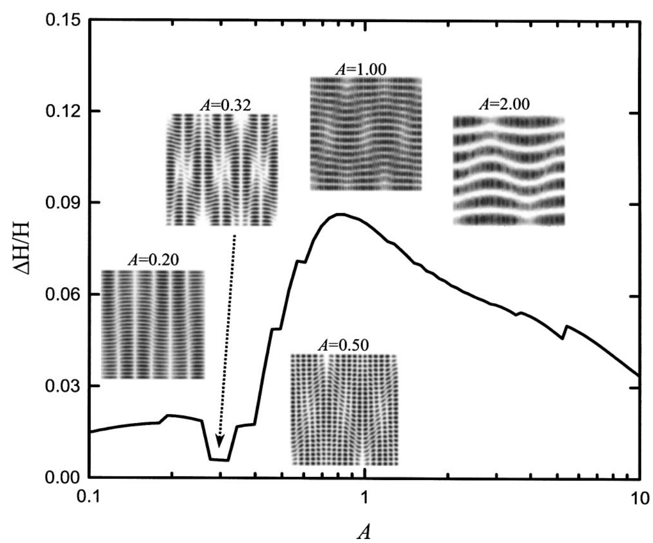

FIG. 3. Similar to Fig. 2 for $\Psi^{3,1}_{29,3}(x,y;A,0.55\pi)$; the calculated pattern with minimum $\Delta H/\langle H\rangle$ corresponds to the experimental result shown in Fig. 1(b).

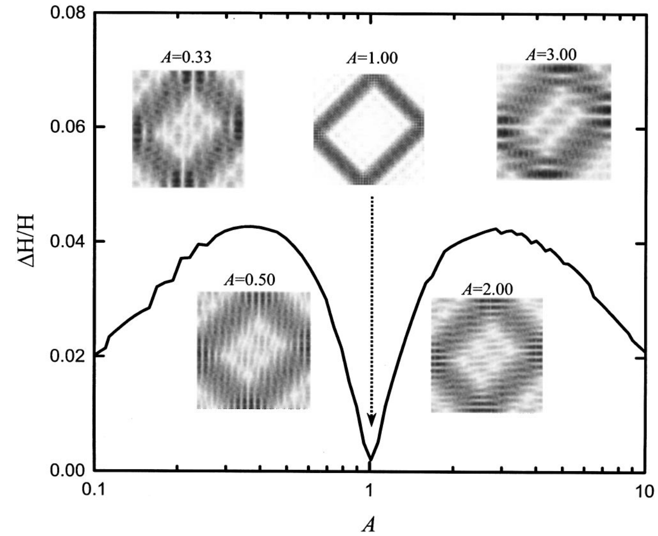

FIG. 4. Similar to Fig. 2 for $\Psi^{1,1}_{80,7}(x,y;A,0.45\pi)$; the calculated pattern with minimum $\Delta H/\langle H\rangle$ corresponds to the experimental result shown in Fig. 1(c).

Since the partially coherent states also often appear in weakly perturbed 2D square billiards [5,6] and in the ballistic quantum dot at resonance [2–4], we use the present model to analyze the resonant-energy states of an open square quantum dot. It can be seen that the theoretical result $\Psi^{1,2}_{40,5}(x,y;2.15,0.5\pi)$ shown in Fig. 5(b) agrees quite well with the representative data of Ref. [4] shown in Fig. 5(a).

Although the specific origin of spontaneous symmetry breaking is still an open question, it is of great value to make a comparison between spontaneous and deliberate symmetry breakings with the present devices. We have fabricated VCSEL's with a ripple boundary to experimentally study the influence of the degree of symmetry breaking. With a considerable ripple boundary, the experimental patterns are always found to be ergodic. Intriguingly, the coexistence of localized and ergodic states is observed in a device with a moderate ripple boundary, as shown in Fig. 6. Even so, the

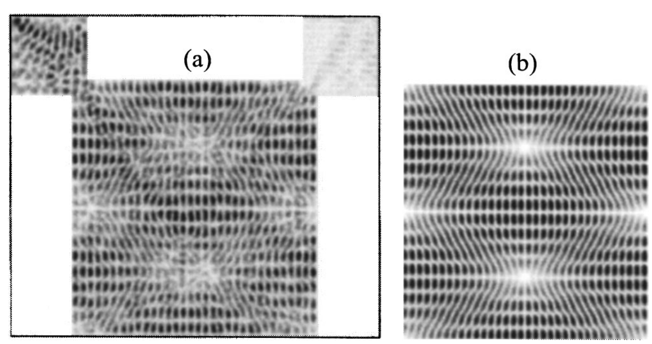

FIG. 5. Comparison of the resonant-energy states of an open square quantum dot with the theoretical result $\Psi^{1,2}_{40,5}(x,y;2.15,0.5\pi)$: (a) resonant pattern from Ref. [4]; (b) the calculated pattern.

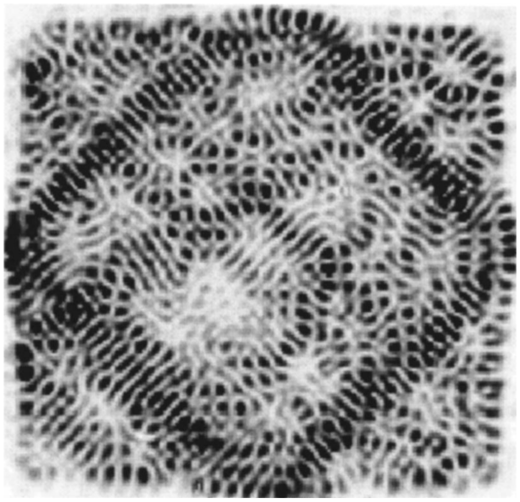

FIG. 6. The experimental near-field pattern of the VCSEL device with a moderate ripple boundary.

partially coherent states localized on the classical orbits are generic and structurally stable in square-shaped VCSEL's without any deliberate symmetry breaking. In brief, a spontaneous symmetry breaking is necessary to lead to the localized states in a square billiard; however, a nonspontaneous one may drive the states into the ergodic regime. Although the quantitative analysis is difficult at the moment, the transition from the localized to ergodic regime is basically consistent with the theoretical analysis of a ripple billiard [5]. A similar transition is also found in the theoretical study of a circular billiard with rough boundaries [16]. It has been numerically shown that the smaller the roughness, the wider the localized regime, even though the state order entering the localized regime becomes higher. In opposition, if the roughness is large to a certain extent, the localized regime is significantly narrowed and the wave function may become utterly ergodic.

Finally, it is worthwhile to connect the present experimental results with similar phenomena discussed in other systems. As a rule, any system is always coupled to some environment and therefore it is never really closed. Nazmitdinov *et al.* [8] have used the effective Hamiltonian to calculate wave functions and coupling coefficients to the environment for the Bunimovich stadium with two attached leads. Their study shows that two types of wave function exist in the open quantum billiard. One type is the short-lived special states that are localized around the classical paths; the other is the long-lived trapped states that are distributed over the whole cavity. Both types of wave function have been observed in the present experiment. Even so, the selection of the states in open systems strongly depends on the condition of the coupling to the environment, as already mentioned in Ref. [8]. In VCSEL devices, the coupling to the environment mostly arises from the vertical mirror. In open quantum dots, however, the coupling is usually through the attached leads. Therefore, the influence of the coupling strength on the localization of the wave functions would be somewhat dissimilar for different open systems.

In summary, the transverse pattern of a microcavity laser has been used to experimentally study the selection rules of spontaneous coherent waves in mesoscopic systems. With the theory of SU(2) coherent states, the spontaneous transverse pattern of a microcavity laser can be described very well. The constraint of minimum energy uncertainty is found to play an important role in selecting the spontaneous coherent states in mesoscopic systems. Moreover, the selection rules are confirmed to be applicable to the resonant-energy states of open square quantum dots.

[1] K. Richter, D. Ullmo, and R. A. Jalabert, Phys. Rep. **276**, 1 (1996).
[2] R. Akis and D. K. Ferry, Phys. Rev. B **59**, 7529 (1999).
[3] I. V. Zozoulenko and K. F. Berggren, Phys. Rev. B **56**, 6931 (1997).
[4] I. V. Zozoulenko, R. Schuster, K. F. Berggren, and K. Ensslin, Phys. Rev. B **55**, R10209 (1997).
[5] W. Li, L. E. Reichl, and B. Wu, Phys. Rev. E **65**, 056220 (2002).
[6] R. Narevich, R. E. Prange, and O. Zaitsev, Phys. Rev. E **62**, 2046 (2000).
[7] Y. H. Kim, M. Barth, H. J. Stöckmann, and J. P. Bird, Phys. Rev. B **65**, 165317 (2002).
[8] R. G. Nazmitdinov, K. N. Pichugin, I. Rotter, and P. Šeba, Phys. Rev. B **66**, 085322 (2002).
[9] T. Blomquist, H. Schanze, I. V. Zozoulenko, and H. J. Stöckmann, Phys. Rev. E **66**, 026217 (2002).
[10] F. von Oppen, Phys. Rev. B **50**, 17 151 (1994).
[11] D. Ullmo, K. Ritcher, and R. A. Jalabert, Phys. Rev. Lett. **74**, 383 (1995).
[12] K. F. Huang, Y. F. Chen, H. C. Lai, and Y. P. Lan, Phys. Rev. Lett. **89**, 224102 (2002).
[13] D. Dragoman and M. Dragoman, Prog. Quantum Electron. **23**, 131 (1999).
[14] V. Doya, O. Legrand, F. Mortessagne, and C. Miniatura, Phys. Rev. Lett. **88**, 014102 (2002).
[15] Y. F. Chen, K. F. Huang, and Y. P. Lan, Phys. Rev. E **66**, 066210 (2002).
[16] K. M. Frahm and D. L. Shepelyansky, Phys. Rev. Lett. **78**, 1440 (1997).